

1 **Oceland: A conceptual model for ocean-land-atmosphere interactions based**
2 **on water balance equations**

3 Luca Schmidt^a, Cathy Hohenegger^a

4 ^a *Max Planck Institute for Meteorology, Hamburg*

5 *Corresponding author:* Luca Schmidt, luca.schmidt@mpimet.mpg.de

6 ABSTRACT: The spatial distribution of precipitation is often misrepresented by General Cir-
7 culation Models (GCM). In particular, precipitation tends to be underestimated over land and
8 overestimated over ocean. One obstacle to resolving this longstanding issue is the lack of a general
9 understanding of land-ocean-atmosphere interactions. More precisely, we do not have a funda-
10 mental theory that tells us which processes or physical quantities determine the partitioning of
11 precipitation between land and ocean. In this study, we investigate whether large-scale constraints
12 on this partitioning exist by using a conceptual box model based on water balance equations. With
13 a small number of empirical but physically motivated parametrizations of the water balance com-
14 ponents, we construct a set of coupled ordinary differential equations which describe the dynamical
15 behaviour of the water vapour content of land and ocean atmospheres as well as the soil moisture
16 content of land. We compute the equilibrium solution of this land-ocean-atmosphere system and
17 analyze the sensitivity of the equilibrium state to model parameter choices. The results show that
18 the ratio of mean land and ocean precipitation rates is primarily controlled by a scale-dependent
19 atmospheric moisture transport parameter, the land fraction, and the permanent wilting point of
20 the soil. We further demonstrate how the proposed model can be adapted for applications on
21 both global and local scales to model, where the latter is useful to study e.g. island precipitation
22 enhancement. For a global scale model configuration with one ocean and one land domain, we
23 show that the precipitation ratio is constrained to a range between zero and one and are able to
24 explain this behavior based on the underlying equations and the fundamental property of land to
25 loose water through runoff.

26 1. Introduction

27 As human beings, we have a great interest in how Earth's climate and its change over time
28 influence living conditions on the land surface. An important question in this respect is how
29 much of the water that evaporates from the Earth's surface will precipitate over land as opposed
30 to over the ocean. Unfortunately, even sophisticated General Circulation Models frequently fail to
31 reproduce observed spatial patterns of precipitation, especially in the Tropics where precipitation
32 amounts are high [Fiedler et al. (2020) and references therein]. However, more fundamentally,
33 we are lacking a theoretical framework in which the partitioning of precipitation between land
34 and ocean can be explained and analyzed with respect to its dependence on properties of the
35 system which may or may not change over time. For instance, is the partitioning sensitive to land
36 size? Do surface characteristics such as soil type matter or is it rather atmospheric conditions that
37 dominate the behavior? It is the aim of this study to introduce a conceptual water balance model
38 that reduces the complexity of the real world to a small number of physical processes that are key
39 for understanding the precipitation partitioning. By investigating the sensitivity of the modelled
40 precipitation partitioning to a variation of the model parameter values, this study can serve as a
41 starting point for filling the gap of theoretical understanding described above.

42 Traditionally, hydrologists separate the Earth's hydrological cycle into an atmospheric branch,
43 describing the sinks and sources of atmospheric moisture, and a terrestrial branch, describe the
44 change of soil moisture [e.g.
45 Peixóto and Oort (1983)]. Evapotranspiration (ET) and precipitation are the links that connect the
46 two branches of the cycle. Since we aim at understanding the precipitation partitioning between
47 land and ocean, it is convenient to choose a different perspective and think about an ocean and
48 a land branch of the water cycle instead. The land and ocean branches are then linked through
49 advective moisture transport between land and ocean atmospheres, and through runoff from the
50 soil to the ocean.

51 The land branch in isolation has been studied intensively since the 1950s. In a pioneering
52 land-atmosphere interaction study by Budyko and Drozdov (1953), the authors describe how an
53 airstream that traverses a region imports atmospheric moisture at the windward contour, moistens
54 or dries depending on the relative magnitude of mean precipitation and ET, and exports moisture at
55 the leeward contour. In this one-dimensional framework known as the Budyko model, precipitation

56 in the region can be expressed as a sum of two components: water that is advected from outside
57 the region and water that previously evaporated from the surface inside the region. The relative
58 contribution of the two components to total precipitation and, hence, the dependence of regional
59 precipitation on advected moisture relative to local recycling through ET, can be expressed as a
60 water recycling coefficient. Important studies that used observations to estimate the water balance
61 components and compute recycling coefficients include Brubaker et al. (1993), who formulated a
62 two-dimensional Budyko model and investigated precipitation recycling in four innercontinental
63 areas and Eltahir and Bras (1994), who focused on the Amazon region and refined the 2D model
64 by allowing for a horizontally heterogeneous precipitation and evapotranspiration field (see Burde
65 and Zangvil (2001) for a comprehensive review of the different adaptations of Budyko's framework
66 and their limitations). A shortcoming of most recycling studies is the dependence of recycling
67 coefficients on the size of the region of interest. The larger the region, the more precipitating
68 water will be derived from within the region. Ent et al. (2010) circumvented this problem by
69 taking a global perspective and defining recycled water as previously evaporated from any point
70 on the land surface and advected water as evaporated from any point on the ocean surface. All
71 mentioned studies show that precipitation recycling contributes significantly to land precipitation,
72 especially in hotspot regions of land-atmosphere interactions such as the Sahel region, the Amazon
73 or mountainous regions in Asia.

74 An alternative to estimating the water balance components from observations is to use analytical
75 parametrizations. In water-limited areas, ET is a function of soil moisture as described by e.g.
76 Manabe (1969) or more recently updated in Seneviratne et al. (2010). Applied to the Budyko
77 recycling framework, this turns the total precipitation into a function of soil moisture, mean
78 advected precipitation, domain size and environmental parameters such as wind speed and potential
79 evapotranspiration. The variability of the latter parameters introduces considerable randomness
80 of precipitation in the real world and limits the utility of the Budyko model when being fixed to
81 constant values. Rodriguez-Iturbe et al. (1991) and Entekhabi et al. (1992) address this issue by
82 modulating mean parametric environmental conditions with Gaussian white noise. Both found
83 that the system preferentially resides in a very dry or very moist soil moisture state for sufficiently
84 high amplitudes of environmental variability. This finding suggests that even such a simple model
85 offers an explanation for hydrological extremes such as droughts in continental regions.

86 What are the physical mechanisms that makes precipitation soil moisture-dependent? Broadly
87 speaking, two lines of arguments were developed. The first one predicts a mostly positive feedback
88 between precipitation and soil moisture, arguing that the enhanced latent heat flux over wet soils
89 favors precipitating convection either through direct water input that can be recycled [e.g. Zangvil
90 et al. (1993)] or by destabilizing the vertical profile in the air aloft [Schär et al. (1999), Findell and
91 Eltahir (2003)]. Hohenegger et al. (2009) points out that the sign of this feedback mechanism can
92 depend on model resolution and the choice of parametrization schemes. The second line of argu-
93 ment explains the soil moisture-precipitation feedback through mesoscale circulations that develop
94 due to different Bowen ratios of wet and dry soil patches Segal and Arritt (1992). Such circulations
95 may drive convective systems from rather moist to rather dry surface areas and contribute to a
96 homogenization of soil moisture [Lynn et al. (1998), Hohenegger and Stevens (2018)]. However,
97 Froidevaux et al. (2014) found that synoptic background winds can also displace convective air
98 from drier soils, where convection was initiated, to wetter soils where the atmospheric conditions
99 favor the onset of precipitation. Hence, the sign of the soil moisture feedback related to mesoscale
100 processes is unclear.

101 The circulation argument has direct implications for our initial question about precipitation
102 partitioning between land and ocean. In the context of Tropical islands, several studies showed that
103 precipitation is enhanced over land due to sea breezes induced by daytime differential heating [Qian
104 (2008), Cronin et al. (2015)]. Even though island precipitation enhancement is often associated
105 with energy balance arguments which are not considered in this work, other factors such as island
106 size [Sobel et al. (2011), Cronin et al. (2015), Wang and Sobel (2017), Ulrich and Bellon (2019)]
107 and background wind speed [Sobel et al. (2011), Wang and Sobel (2017)] seem to matter, too, and
108 these factors might be independent of the occurrence of sea breezes. We will return to the case of
109 islands in the last part of this paper and explore what a purely water balance based approach can
110 teach us about precipitation enhancement in such small-scale systems.

111 **2. Model description**

112 In this study, we want to understand the controlling factors for precipitation partitioning between
113 land and ocean. Specifically, we ask whether fundamental constraints for this partitioning arise
114 from water balance equations. To this end, we propose a box model as sketched in Figure 1 with

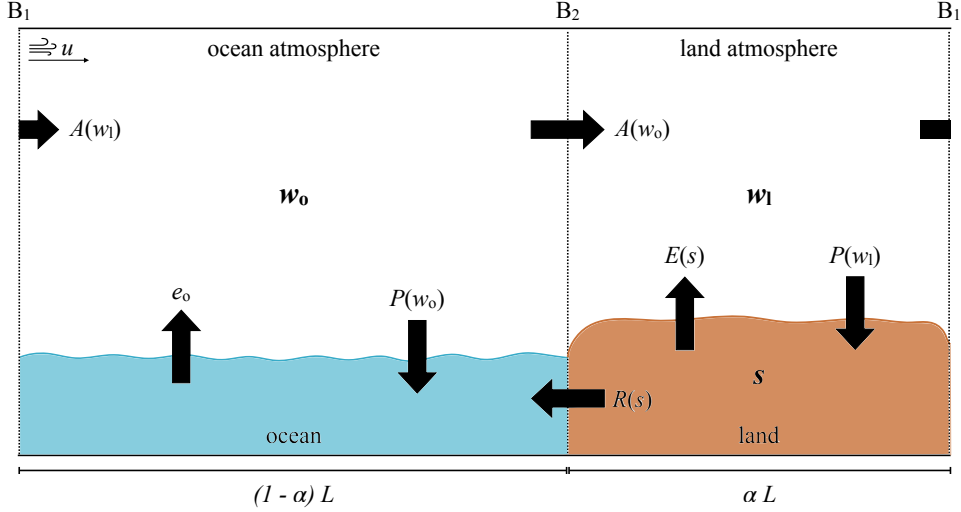


FIG. 1. Closed model sketch and water vapor pass distribution.

115 an ocean domain, denoted by subscript ‘o’, and a land domain, denoted by subscript ‘l’. The
 116 relative size of the two domains is given by the land fraction parameter α . Each of the two domains
 117 contains a ground box at the bottom (ocean or land) and an atmospheric box aloft. While the
 118 horizontal extent of the model is prescribed by length L , the downward/upward vertical extent of
 119 the ground/atmospheric boxes is taken to be infinite. The model has periodic boundary conditions,
 120 i.e. topologically, it resembles the wall of a cylinder with the right boundary of the land domain
 121 connecting to the left boundary of the ocean domain. This turns the model into a closed system
 122 in which water is conserved and which does not interact with any external environment. Such a
 123 *closed* model (CM) can be used to describe, for example, the entire globe or the full Tropics if
 124 net water exchange with the Extratropics can be assumed to be negligible. Later, in section 5, we
 125 introduce an *open* model (OM) formulation suitable for regional systems in which case boundary
 126 values are provided by synoptic-scale conditions and the modelled area can act as a net sink or
 127 source of moisture. In this case, water is still conserved in a global sense but not necessarily within
 128 the model.

129 a. Water balance equations

130 We further assume that the model boxes have well-mixed properties and that all water fluxes
 131 between them can be expressed as functions of their mean moisture content, i.e. the moisture state

of the boxes. For atmospheric boxes, we use the mean integrated water vapour pass w in mm, and for the land box the unitless mean relative soil moisture saturation s to describe the moisture state. As the ocean is considered fully saturated at all times, we don't need to assign a moisture variable to it. Hence, the full information on the moisture state of the model at any given moment in time t is given by the set of state variables $\{w_o(t), w_l(t), s(t)\}$.

Following earlier studies by Peixóto and Oort (1983) and Brubaker et al. (1991), we describe the time-evolution of the state variables by coupled water balance equations in which moisture sinks and sources are represented by water fluxes between the boxes:

$$\frac{ds}{dt} = \frac{1}{nz_r} [P(w_l) - R(s, w_l) - E(s)] \quad (1)$$

$$\frac{dw_l}{dt} = E(s) - P(w_l) + A_l(w_l, w_o) \quad (2)$$

$$\frac{dw_o}{dt} = e_o - P(w_o) + A_o(w_l, w_o). \quad (3)$$

The relevant fluxes, which are indicated by black arrows in Figure 1, are precipitation P from atmosphere to ground boxes, evapotranspiration E from soil to land atmosphere, ocean evaporation e_o to the ocean atmosphere, runoff R from soil to ocean and advection A between the atmospheric boxes. All fluxes are given as spatio-temporal mean flux rates in mm/day ('mean' being frequently omitted in the remainder of this text). This is, in order to obtain the total moisture change in mm²/day, Equations (1) and (2) would need to be multiplied by land domain size αL and Equation (3) by ocean domain size $(1 - \alpha)L$. The advection terms A_l and A_o refer to the *net* advection rate into the land and ocean atmosphere, respectively, and are positive for a net moisture import and negative for net moisture export. Dimensionless soil porosity n , hydrologically active soil depth z_r in mm and e_o are constant model parameters. An implicit assumption of this water balance approach is that the water holding capacity of the atmosphere does not change significantly over long enough timescales which we consider here.

b. Parametrizations

While the conservation of water is a rather fundamental condition, there are no simple fundamental laws governing the water fluxes between the model boxes. Instead, we need to turn to empirical

relationships between the flux quantities and moisture state variables, as has been previously done by Rodriguez-Iturbe et al. (1991). We adopt their parametrization of runoff as the fraction R_f of precipitation that does not infiltrate the soil but instead returns to the ocean in the form of surface or sub-surface currents. The runoff fraction,

$$R_f(s) = \epsilon s^r, \quad (4)$$

contains two empirical dimensionless parameters $\epsilon \approx 1$ and $r \approx 2$. It tells us that runoff intensifies as the soil moistens. The complete expression for the runoff rate reads

$$R(s, w_1) = R_f(s)P(w_1), \quad (5)$$

but it proves to be convenient to combine precipitation and runoff in Eqn. (1) to $P(w_1) - R(s, w_1) = P(w_1)\Phi(s)$, where we introduced the infiltration function $\Phi(s) = 1 - R_f = 1 - \epsilon s^r$. Note, that this parametrization assumes that runoff discharge happens uniformly across the land domain and that its water does not participate in any secondary processes that could moisten the soil.

For precipitation, Rodriguez-Iturbe et al. (1991) follow the approach by Budyko and Drozdov (1953) and obtain an expression for precipitation that is dependent on soil moisture. However, the Budyko approach assumes the advected precipitation component to be known and set to a fixed value which is not a desirable construction in our case where precisely the interaction of land and ocean through advection is one main focus. Instead, we use the empirical parametrization established by Bretherton et al. (2004). The authors find that the precipitation rate over tropical oceanic regions shows an exponential relationship with the mean water vapor pass,

$$P(w) = \exp \left[a \left(\frac{w}{w_{\text{sat}}} - b \right) \right]. \quad (6)$$

The parametrization introduces three parameters, two empirical dimensionless parameters $a \approx 15.6$ and $b \approx 0.6$ and the saturated water vapor pass w_{sat} in mm. Lacking a corresponding expression for extratropical ocean regions and land in general, we make the explicit assumption that Equation (6) holds everywhere. This assumption is rather crude and has major implications for the results presented in Section 4 as will be discussed in greater detail later. Furthermore, the same saturation

177 water vapor pass is assumed over land and over ocean, implying similar energetic conditions across
 178 the entire model domain.

179 The qualitative dependence of evapotranspiration (ET) on soil moisture saturation is long-known,
 180 see e.g. Budyko (1956) or more recently and slightly modified in Seneviratne et al. (2010). ET
 181 is close to zero for soil moisture saturation values below the permanent wilting point, $s < s_{\text{pwp}}$,
 182 increases approximately linearly in a transition range between the permanent wilting point and a
 183 critical value close to the field capacity, $s_{\text{pwp}} < s < s_{\text{fc}}$, and reaches a plateau for higher s -values,
 184 $s > s_{\text{fc}}$, where evapotranspiration is nearly constant. The evapotranspiration value of the plateau
 185 is denoted by E_p . It is an energy-dependent parameter that increases with increasing radiative
 186 energy input. In this work, E_p will be set to a constant value. For computational convenience,
 187 we parametrize evapotranspiration by the following smooth function which has the qualitative
 188 properties described above,

$$E(s) = \frac{E_p}{2} \left[\tanh \left(10 \left(s - \frac{s_{\text{pwp}} + s_{\text{fc}}}{2} \right) \right) + 1 \right]. \quad (7)$$

189 This parametrization implies that the entire land box is either covered by a single vegetation type
 190 or that a combination of vegetation types can be modelled by means of an effective mean value of
 191 s_{pwp} , s_{fc} and E_p .

192 It remains to find expressions for the *mean net* advection rates into the land and ocean atmospheres,
 193 hereafter just land/ocean advection rates. The net total advection flux into a given box is the
 194 difference between the moisture entering and leaving the box per unit time. This moisture transport
 195 is driven by a mean background wind velocity u which we assume to be constant across the model
 196 domain. Total advection in mm^2/day can then be expressed as

$$A_{\text{tot}} = (w_{\text{in}} - w_{\text{out}})u. \quad (8)$$

197 The assumed water vapour pass distribution is characterized by one value w_o across the ocean
 198 atmosphere and another value w_l across the land atmosphere. Hence, wind transports the moisture
 199 amount $w_o u$ into the land domain and $w_l u$ into the ocean domain. Since we only have two boxes
 200 and periodic boundary conditions, the total net advection rate A_{tot} into the land and ocean domains
 201 are identical in magnitude but with opposite signs. If the ocean has a net advective outflux, then

TABLE 1. Parameter ranges for closed model Monte Carlo simulations with uniform sampling.

Parameter	Minimum	Maximum	Range choice motivated by
s_{pwp}	0.2	0.54	Hagemann and Stacke (2015)
s_{fc}	0.5	0.84	Hagemann and Stacke (2015)
e_{p} [mm/day]	4.1	4.5	Rodriguez-Iturbe et al. (1991)
nZ_{T} [mm]	90.0	110.0	Rodriguez-Iturbe et al. (1991)
e_{o} [mm/day]	2.8	3.2	C. Hohenegger, private communications
ϵ	0.9	1.1	Rodriguez-Iturbe et al. (1991)
r	2.0	2.0	fixed due to computational method, Rodriguez-Iturbe et al. (1991)
a	11.4	15.6	Bretherton et al. (2004)
b	0.522	0.603	Bretherton et al. (2004)
w_{sat} [mm]	65.0	80.0	Bretherton et al. (2004)
α	0.0	1.0	full possible range
u [m/s]	1.0	10.0	reasonable range for lower tropospheric mean wind speed
L [km]	1000.0	40000.0	chosen to represent different length scales
$\tau = u/L$ [day $^{-1}$]	0.00216	0.864	computed from extreme u and L

the land atmosphere gains this moisture as net advective influx. In a last step, this total advection rate needs to be translated into mean advection rates per unit land/ocean length, i.e.

$$A_1 = \frac{(w_o - w_l)u}{\alpha L} \quad (9)$$

and

$$A_o = -\frac{(w_o - w_l)u}{(1 - \alpha)L}, \quad (10)$$

where A_1 and A_o have units mm/day and α and L are the land fraction and full model length, respectively, as introduced earlier.

With these parametrizations, the model has a total of 14 free parameters which we can reduce to 12 if we treat nZ_{T} in mm as one combined parameter and introduce the characteristic rate of atmospheric transport $\tau = u/L$ in day $^{-1}$. Table 1 provides sensible ranges for the 12 parameters. These ranges are used to constrain the precipitation ratio across the parameter space and test the sensitivity of the model results to parameter variations.

3. Evaluation methods

In this section, we present the analysis methods that are employed to evaluate the model behavior and assess the sensitivity of the precipitation ratio to a variation of the model parameters.

215 The focus of the present study lies on the properties of equilibrium states of the modelled system.
 216 The equilibrium solution to the model equations (1) to (3) has to be found numerically. We use
 217 the `DynamicalSystems.jl` library from Datseris (2018) to find all roots of the model equations
 218 and determine whether each root represents a stable or unstable fixed point of the system. With
 219 the equilibrium soil moisture and water vapour pass values obtained in this way, we can compute
 220 all fluxes and flux ratios of interest using the parametrizations introduced in Section 2.b.

221 Adopting an agnostic view on the plausibility of different combinations of parameter values
 222 from the ranges given in Tab. 1, we are confronted with a 12-dimensional parameter space with
 223 uniform probability distribution. A general assessment of the sensitivity of equilibrium states and
 224 related quantities to a variation of the model parameters requires a sampling of the full parameter
 225 space. To this end, we perform $n = 10000$ model simulations for randomly chosen combinations
 226 of parameter values, each yielding a corresponding fixed point.

227 Having obtained a sufficiently large dataset in this way, the sensitivity of a computed quantity
 228 Q to a given parameter p can be visually and quantitatively evaluated with Q - p scatter plots. The
 229 sensitivity is given by the correlation between Q and corresponding p values. For a potentially
 230 non-linear and non-monotonic distribution of the data points, a suitable sensitivity measure is the
 231 mutual information $MI(p, Q)$ which quantifies how much knowing the value of p will reduce the
 232 uncertainty about Q . Mutual information MI is computed as,

$$MI(p, Q) = H(p) + H(Q) - H(p, Q), \quad (11)$$

233 where $H(p)$, $H(Q)$ and $H(p, Q)$ are the information entropies [Shannon (1948)] of p and Q values
 234 and their joint distribution, respectively, where we use amplitude binning to ascribe probability
 235 distributions. We follow an approach by Datseris and Parlitz (2022) to assess the significance level
 236 for an obtained sensitivity value and to compare the sensitivity of different parameters p_i . To this
 237 end, we define a mutual information index

$$I_{MI}(p_i) = \frac{MI(\hat{p}_i, Q)}{MI_{\text{uncorr}, 3\sigma}(\hat{p}_i, Q)}, \quad (12)$$

238 where \hat{p}_i denotes a rescaled version of p_i with values between 0 and 1 and $MI_{\text{uncorr}, 3\sigma}(\hat{p}_i, Q)$
 239 is the mutual information value that deviates by three standard deviations σ from the mean of

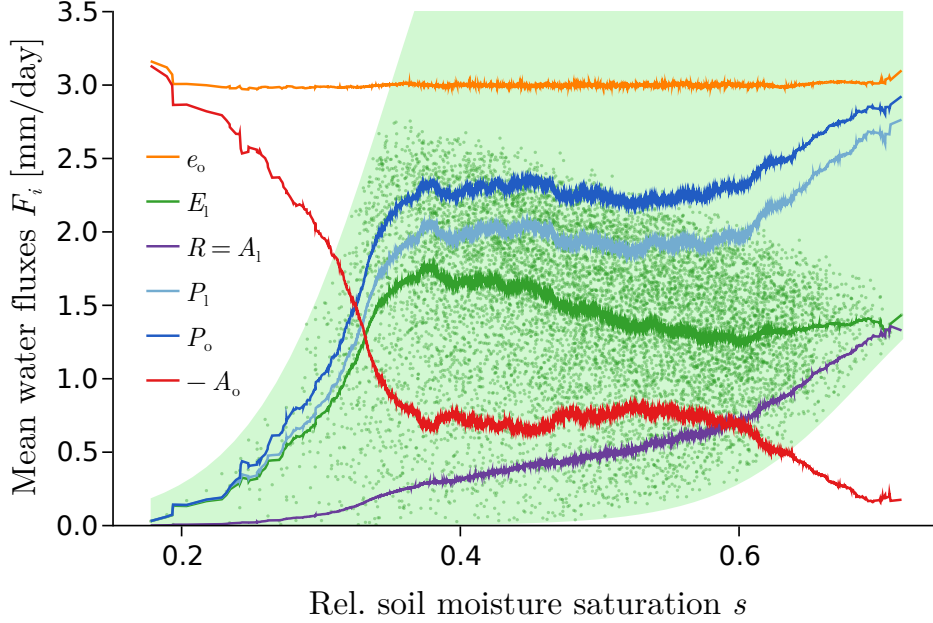


FIG. 2. Symmetric rolling average of equilibrium fluxes versus soil moisture saturation computed from CM data. For evapotranspiration (green line), the individual data points are shown as scatter plots and the range of $E_1(s)$ parametrizations for different parameter combinations is shaded in light green.

a distribution of MI values for uncorrelated \hat{p}_i and Q . A detailed description of this method is presented in Appendix [***]. $I_{MI} = 1$ is used as the significance threshold and the higher $I_{MI}(p_i)$, the more sensitive Q is to a variation of parameter p_i .

4. Closed model results

The results presented in this section are based on the data of 10000 simulations of the closed model which randomly sampled the parameter space as explained in Section 3, each yielding the equilibrium solution for a unique point in the parameter space provided in Table 1. The obtained dataset will henceforth be referred to as "CM data". The section is organised in two parts. First, we discuss basic features of the model and their implications for the partitioning of precipitation between land and ocean. Second, we examine to which parameters the precipitation ratio is most sensitive and which physical arguments explain these individual relationships.

251 *a. Basic model behaviour*

255 Figure 2 shows rolling averages of the equilibrium flux rates of land precipitation P_l , ocean
 256 precipitation P_o , ocean evaporation e_o , evapotranspiration from the land surface E_l , runoff R and
 257 land and ocean advection, A_l and A_o , respectively, over the attained soil moisture saturation values
 258 s . Note, that the ocean advection rate A_o has negative values for all equilibrium solutions and is
 259 therefore multiplied by -1 to simplify the comparison of its magnitude with other fluxes. The
 260 figure displays averaged equilibrium data from all different parameter combinations. This is, one
 261 should not confuse the plotted curves with well-defined functions of s with fixed parameter values.
 262 Rather, Figure 2 contains the combined information from all model runs. To illustrate this point
 263 more clearly, some additional information is plotted for evapotranspiration E_l which is an explicit
 264 function of s according to Equation (7): The green shaded area marks the range of different
 265 realisations of Eqn. (7), covering different combinations of values for s_{pwp} , s_{fc} and E_p . The small
 266 green dots are the actual equilibrium data points which lie somewhere on their corresponding
 267 realisation of Eqn. (7). The moving average is then computed from these data points and gives the
 268 green solid line for E_l . Even though the averaged flux rates mask the diverse interplay of different
 269 parameters, we can use them as a starting point for the following discussion and appreciate three
 270 qualitative observations which, as we will see, do not require a deeper understanding of parameter
 271 interactions to obtain important insights into the model behavior and draw first conclusions about
 272 precipitation partitioning:

- 273 1. Land advection, A_l (purple line) is strictly positive, i.e. moisture is supplied by the ocean
 274 atmosphere to the land atmosphere.
- 275 2. Land advection A_l and runoff R are identical in magnitude. Combined with the first observa-
 276 tion, this means that all water loss through runoff is compensated by advection.
- 277 3. All flux rates are bound to the open interval $(0, e_o)$, i.e. no other mean flux rate can become
 278 larger than the ocean evaporation rate (orange line).

279 The first observation shows a clear directionality of net atmospheric moisture transport from the
 280 ocean to the land for the system in equilibrium. Going back to Equation (9), this is equivalent to
 281 the statement that the ocean atmosphere is moister than the land atmosphere, i.e. $w_o > w_l$. This

282 has direct implications for the partitioning of precipitation between land and ocean. Here and in
 283 the remainder of this work, we will quantify this partitioning with the precipitation ratio,

$$PR = \frac{P_l}{P_o} = \frac{P(w_l)}{P(w_o)}. \quad (13)$$

284 The precipitation parametrization $P(w)$ from Equation (6) is a monotonically increasing function
 285 of water vapor pass w , meaning that a moister atmosphere results in stronger precipitation. As we
 286 use this equation to describe both ocean and land precipitation, a moister ocean atmosphere will
 287 produce higher precipitation than the drier land atmosphere. As a consequence, the precipitation
 288 ratio is bound by an upper limit of one, i.e $PR < 1$.

289 The second observation that advection equals runoff can be understood in two steps. First, we
 290 know from the soil moisture balance of Eqn. (1) that

$$P_l = E_l + R \quad (14)$$

291 when the soil moisture attains a constant value, i.e. when $ds/dt = 0$. Second, we can return to
 292 the Budyko framework Budyko and Drozdov (1953) discussed in the introduction and express
 293 the land precipitation as the sum of advected precipitation P_a and a contribution from local
 294 evapotranspiration P_e . The former corresponds to the difference of incoming advected moisture
 295 $A_{in} = w_o u$ and some part of this incoming moisture that just traverses the land domain without
 296 precipitating and leaves on the leeward side, A_{out} . The latter is the difference of the total evaporated
 297 moisture, $E_{in} = \alpha L E_l$, and some part of this evaporated moisture that is carried out of the land
 298 domain on the leeward side, E_{out} . The two outgoing moisture fluxes A_{out} and E_{out} together make
 299 up the total outgoing moisture $w_l u$. In effect, these considerations can be combined to

$$\begin{aligned} P_l = P_a + P_e &= \frac{A_{in} - A_{out} + E_{in} - E_{out}}{\alpha L} \\ &= E_l + \underbrace{\frac{(w_o - w_l)u}{\alpha L}}_{A_l}, \end{aligned} \quad (15)$$

300 where the division by αL was necessary to create spatial mean rates analogous to the procedure
 301 explained in section 2 b. When comparing Eqn. (14) to Eqn. (15), it becomes clear that runoff and

advection have the same magnitude. If we imagine a system without advection, e.g. because the land and ocean atmosphere were separated by an impenetrable barrier, runoff would continuously reduce the soil moisture saturation and with it the evapotranspiration and precipitation fluxes. Eventually, the system would attain the trivial equilibrium solution $\{s = 0, w_1 = 0\}$. On the ocean side of this hypothetical system, equilibrium conditions would be rather moist with w_o such that $P_o(w_o) = e_o$. We conclude that it is the fundamental property of land to lose water in the form of runoff that requires a net atmospheric moisture import of the same magnitude for any nontrivial equilibrium solution.

The explanation of the third observation, that all flux rates are smaller e_o , is now rather straightforward: Ocean precipitation P_o needs to be smaller than e_o since some of the evaporated water is exported to the land and therefore no longer available for precipitation. Since the land atmosphere is drier than the ocean atmosphere, it follows that $P_l < P_o < e_o$, and consequently also the components of land precipitation, namely E_l , R and A_l from Eqns. (14) and (15), each need to be smaller than e_o . Lastly, ocean advection which describes the export of moisture from the ocean atmosphere must be smaller than e_o because no more than the moisture input from the ocean surface can be exported.

Note: Everything below has not yet been reworked. So you don't need to read any further :) My plan however is to continue with briefly describing the shape of the fluxes in Fig. 2, pointing out that there seem to be three regimes: For low s , precipitation (blue lines) follows land evapotranspiration (green line) fairly closely while runoff/advection (purple line) is negligible. For intermediate s , precipitation rests in a plateau phase in which decreasing E_l is balanced by increasing runoff/advection. For highest s , precipitation is eventually dominated by runoff/advection. This behaviour cannot be understood by looking at the parametrisations or model equations alone. Rather, the influence of different parameters is encoded in it (e.g. low s values correspond to high α , highest s values share a high permanent wilting point etc.). This will be my link to the next section of the results, i.e. parameter sensitivities. I don't know if this will work out but ideally, I would like to briefly return to Fig. 2 after having discussed the dominant parameter sensitivities and piece things together, so that the reader understands why the fluxes in Fig. 2 look the way they do.

The behaviour of the fluxes for different soil moisture values in Figure 2 can be roughly divided into three regimes. The first regime extends from the lowest soil moisture values up to about $s \approx 0.35$ and is characterized by a sharp

b. Parameter sensitivity of PR

Building on the preceding general description of the model behavior, we now draw our attention to the sensitivity of the precipitation ratio with respect to a variation of different model parameters. Three parameters stand out in having a particularly strong impact on PR : Land fraction α , atmospheric moisture transport parameter τ and permanent wilting point s_{pwp} . We discuss the underlying relationships using the same CM data as before.

Land fraction α : Figure 4 shows a scatter plot of PR values over α . Despite considerable spread in PR , we can see that $PR \rightarrow 1$ for both limits, $\alpha \rightarrow 0$ and $\alpha \rightarrow 1$. This reflects very similar moisture conditions in the two atmospheres when α is extreme. Knowing that $w_o > w_l$ for all equilibrium states, it follows that PR will only decrease if $\Delta w = w_o - w_l$ increases. As has been discussed in the preceding section, the system's equilibrium states for a tiny land domain are relatively moist. For $\alpha \rightarrow 0$, a large Δw cannot be sustained since the resulting advection amount $\Delta w u$ would translate to a large land advection rate, $\Delta w u / (\alpha L)$, that would immediately moisten the land atmosphere and assimilate w_o and w_l . On the other end of the range, when the ocean is tiny, i.e. $\alpha \rightarrow 1$, large moisture differences are likewise impossible: This time, Δw is limited by the total amount of water that enters the system through the ocean surface. The ocean atmosphere cannot export more water than it receives. Therefore, the total amount of evaporated water sets the upper limit for advection, $\Delta w u < (1 - \alpha) L e_o$. This amount decreases with increasing α , so that Δw needs to decrease with it. Moreover, Δw needs to stay below this limit since the ocean atmosphere has to stay moister than the land atmosphere to facilitate advection in the first place.

Along the mid- α range, PR decreases until it reaches a minimum beyond which the ratio increases again. This behaviour is somewhat concealed by the large spread in PR for intermediate land fractions but is both visible in the means of bins of 100 consecutive α values (dark grey line) and in graphs for which all parameters except α were kept fixed (not shown). A mathematically rigorous analysis of $PR(\alpha)$ in this range and, in particular, the location of the minimum is difficult

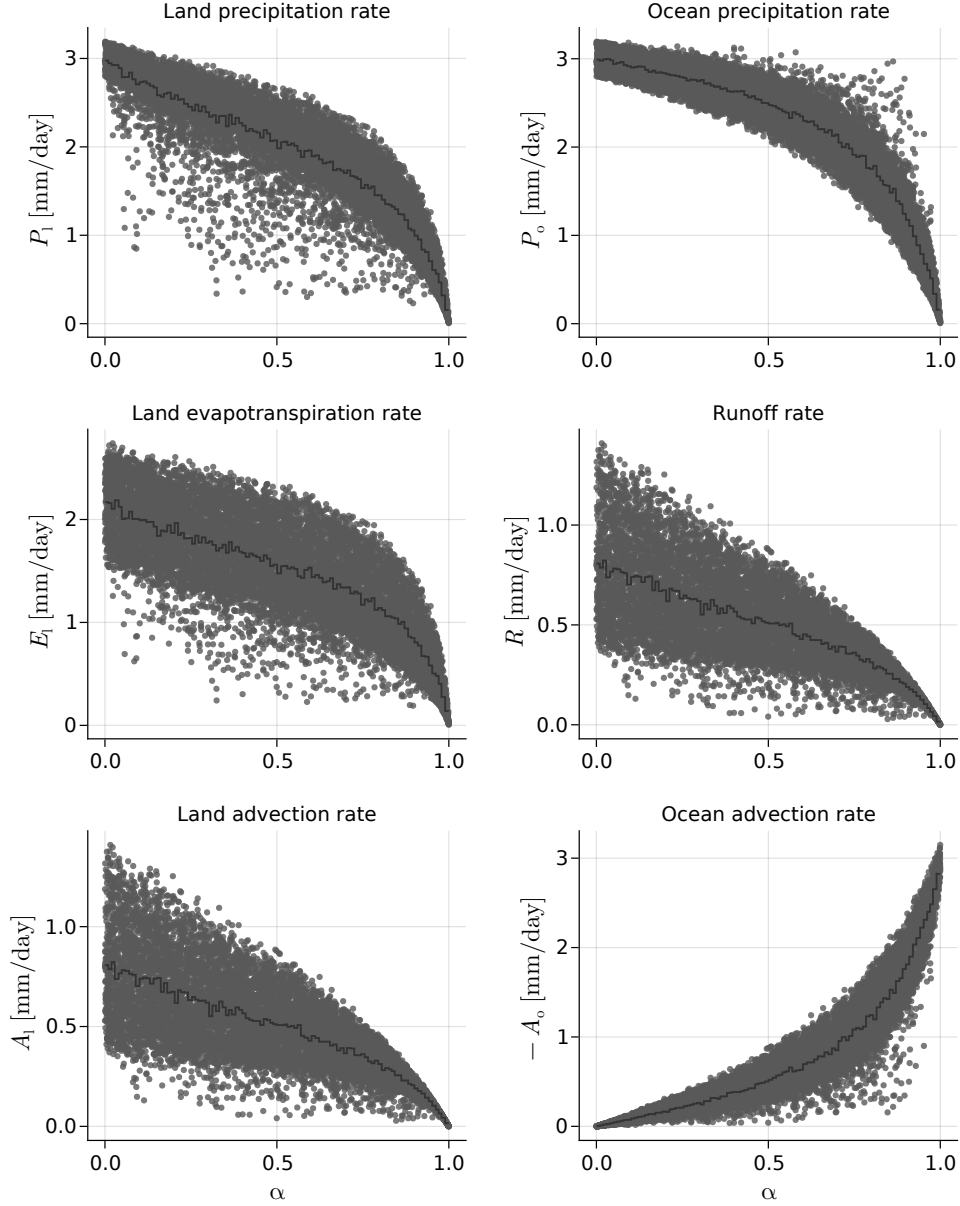


FIG. 3. Mean water fluxes computed from the equilibrium states of 10000 closed model runs with randomly sampled parameter values and plotted over land fraction α . The dark grey line shows the mean values of bins of 100 consecutive α -values. The negative ocean advection rate A_o reflects a net transport of water out of the ocean and into the land atmosphere. Multiplication by -1 simplifies the comparison of its magnitude with the other flux quantities.

due to the lack of an analytical expression for the relationship between precipitation ratio and land fraction. We can write,

$$PR(\alpha) = \frac{P_l(\alpha)}{P_o(\alpha)} = \frac{E_l(s) + \frac{(w_o - w_l)u}{\alpha L}}{e_o - \frac{(w_o - w_l)u}{(1-\alpha)L}}, \quad (16)$$

but we may not overlook the fact that our state variables are implicit functions of α , too, i.e. $s(\alpha)$, $w_o(\alpha)$ and $w_l(\alpha)$. Even though we don't know the analytical form of these state variable dependencies, Eqn. (4) gives a useful indication of why the precipitation ratio should decrease for small but increasing α and why it should increase again as α approaches one. This indication lies in the factors $f = 1/\alpha$ and $g = 1/(1-\alpha)$ in the land and ocean advection rates, respectively. Assuming that the system resides in an equilibrium state for some α close to zero, a small increase in α would lead to a rather strong drop in the land advection rate (strong negative slope of f at low α) compared to the rather mild increase in the magnitude of ocean advection (weakly positive slope of g at low α)...

I stopped here because I wondered if it makes sense to explain the shape of $PR(\alpha)$ in such great detail. Maybe all this could be described in a much simpler way by starting from total moisture input rather than mean rates. The argument would go something like this: increasing land = generally less water available to the circulation in the system. Consequently, the moisture state as a whole must become drier, i.e. all state variables decrease but at different rates. Land precip (and with it w_l) decrease both through a reduction of E_l and a rather sharp drop in A_l due to factor f . Ocean precip only decreases by slight increase of $-A_o$. For large α the system is already in a rather dry state. E_l decreases only slightly with decreasing s and impact of f is less strong. For ocean precip, the opposite is true. Here, g plays a stronger role now and increases the ocean advection rate strongly. In the end, the interplay of the different nonlinear parametrisations make the behaviour of PR asymmetric around $\alpha = 0.5$ and hard to understand in detail.

Atmospheric rate of transport τ : The ratio between mean horizontal wind speed and spatial extent of the model, $\tau = u/L$, is a measure for the efficiency with which moisture is transported across the model atmosphere. Its inverse value, τ^{-1} , corresponds to the time that an air parcel would need to travel across the full domain length L . In the advection terms of Eqn. (2) and (3), τ appears as the rate at which moisture is moved across the boundaries between the two atmospheric boxes. It has therefore major implications for the ability of advection to assimilate the moisture conditions over ocean and land. A very small value of τ , i.e. a low rate of transport, corresponds

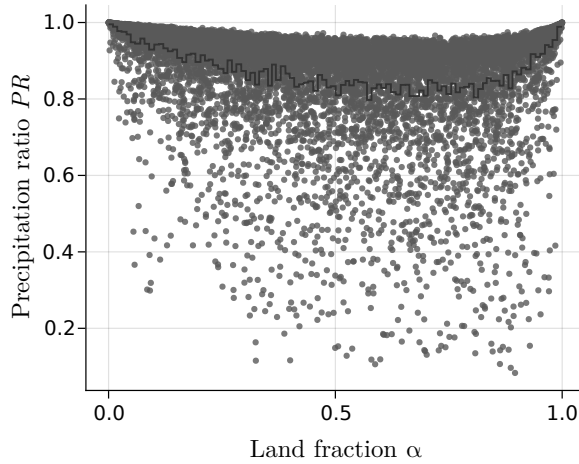


FIG. 4. Smile plot

393 to a combination of large domain size and low wind speed while a small domain and strong wind
 394 result in a very large value of τ . Assuming a fixed land fraction α , a larger moisture difference
 395 Δw is needed to move the same total amount of water across a box boundaries when the rate of
 396 transport is small, compared to when it is large. Except for the special cases of extreme land
 397 fractions, $\alpha \rightarrow \{0, 1\}$, where α enforces very similar moisture conditions over land and ocean, it is
 398 primarily τ that sets the moisture difference which is needed to attain the equilibrium state. This
 399 dominant role is illustrated in Figure 5 which shows the scatter plot of precipitation ratio over τ .
 400 While we already assessed that α sets the overall upper limit of PR , Fig. 5 shows that τ sets the
 401 overall lower bound. It explains the large spread for PR values in the mid- α range in Figure 4,
 402 where the efficiency of atmospheric moisture transport is particularly important. Only high rates
 403 of transport enable the system to attain an equilibrium state with rather similar moisture conditions
 404 over land and ocean. For instance, if $\tau > 0.4 \text{ day}^{-1}$, then PR stays above 0.8 regardless of the choice
 405 of values for other parameters. Note, that τ combines the information about both wind and spatial
 406 extent of the model. If one fixes one of the two, e.g. $L = 40000 \text{ km}$ to simulate the full Tropics
 407 along the equator, the physically sensible range of τ is limited. For example, in order to obtain
 408 a rate of transport larger than 0.4 day^{-1} , such a large L would require a minimum wind speed of
 409 185 m/s , a value that lies beyond the highest wind speed ever measured on Earth. More realistic
 410 mean wind speed values for such a large domain could lie around 5 to 10 m/s with corresponding
 411 rates of transport, $\tau \approx 0.01 - 0.02$. At these low values of τ , the spread of PR values is considerable

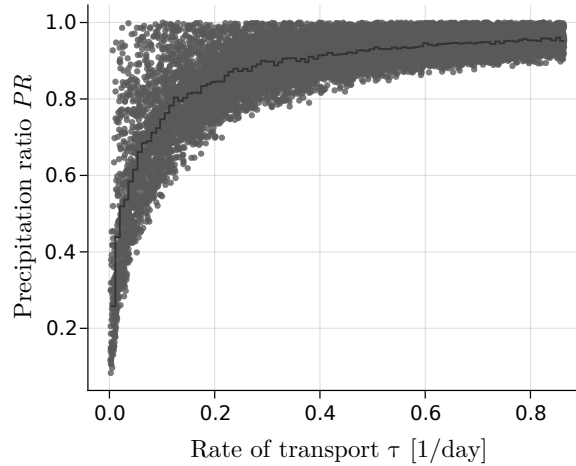


FIG. 5. τ -dependence

which means that also other parameters have a substantial influence on the attained equilibrium state.

Permanent wilting point s_{pwp} : It takes work to extract water from the soil and the drier the soil, the more work is needed to facilitate evapotranspiration. Regardless of whether the land surface is bare or covered with vegetation, s_{pwp} is a characteristic property of the soil type which denotes the relative soil moisture saturation value below which practically no water can be extracted. The left panel of Figure 6 shows the parametrization function of evapotranspiration, $E_1(s)$, for different choices of the permanent wilting point. For instance, $s_{\text{pwp}} \approx 0.3$ might correspond to loam and $s_{\text{pwp}} \approx 0.5$ to clay (Hagemann and Stacke (2015)). In the evapotranspiration graphs, s_{pwp} determines the soil moisture value at which the curve transitions from $E_1 \approx 0$ to the regime of steeply increasing E_1 . Since the field capacity s_{fc} lies $\Delta s = 0.3$ higher than s_{pwp} for all relevant soil types, a change in s_{pwp} merely shifts the evapotranspiration graph along the s -direction, while its shape remains unchanged.

Figure 7 shows a negative trend of the precipitation ratio with increasing s_{pwp} for the performed model runs. The impact of soil type on the precipitation ratio is weaker than, for example, the impact of τ but it is nonetheless clearly visible and s_{pwp} represents the third most sensitive model parameter. To understand the dependence of PR on s_{pwp} , it is convenient to think of a system in equilibrium for some permanent wilting point, e.g. $s_{\text{pwp}} = 0.3$. The mean equilibrium soil moisture value in the CM data for $s_{\text{pwp}} = 0.3$ is $s = 0.43$. This initial state of the model is displayed

431 as a blue dot in Figure 6. An abrupt increase of s_{pwp} to $s_{\text{pwp}} = 0.4$ leads to a significant drop
 432 of E_1 as illustrated by the first red arrow connecting the blue and green dot in the left panel of
 433 Fig. 6. The green dot represents a temporary state where the model is not in equilibrium because
 434 the state variables have not yet adapted to the new situation. At this point, the soil receives the
 435 same amount of precipitation but loses less water through evapotranspiration. As a result, the soil
 436 moistens. As time progresses, the system attains a new equilibrium state at a higher s value which
 437 is marked by the orange dot. This moistening of the soil is shown in the right panel of Fig. 6,
 438 where the equilibrium s values of the CM data are plotted over the corresponding values of s_{pwp} .
 439 However, as s increases, runoff and land advection rate increase, too. Assuming that $\tau/(\alpha L)$ is
 440 kept fixed, Δw has to increase to facilitate the increase of advection. The water that is supplied
 441 to the land atmosphere as advection is taken from the ocean atmosphere, where w_o decreases as a
 442 consequence. Hence, an increase in advection is only possible, if w_l decreases more strongly than
 443 w_o . The increase in R combined with a decrease in P_l is the reason why the new equilibrium state
 444 for $s_{\text{pwp}} = 0.4$ will have a moister soil but a lower evapotranspiration rate than the initial state for
 445 $s_{\text{pwp}} = 0.3$. The fact that w_l must decrease more strongly than w_o in the adaptation process is the
 446 reason why PR declines with increasing s_{pwp} .

452 **5. Open model formulation**

453 The closed model discussed so far can be applied to any system for which the total net advection is
 454 zero. Such conditions might be met in the real world when we look at very large scales, e.g. global
 455 domains such as the tropical band. However, in the case of more local, small scale phenomena, the
 456 net advection might not be zero and the situation is better captured by an open model configuration,
 457 where moisture inflow at the windward model boundary is a model parameter and no constraints
 458 apply to the moisture outflow at the leeward boundary. In this model configuration, the modelled
 459 domain can have a net advection larger or smaller than zero. In the following, we present the
 460 formalism and analysis of an open model with two oceanic domains and an island inbetween them.

461 *a. Open model equations*

462 The model equations for an open configuration are similar to the ones for the closed model. This
 463 time, four instead of three equations are needed as the system has now one more ocean domain.

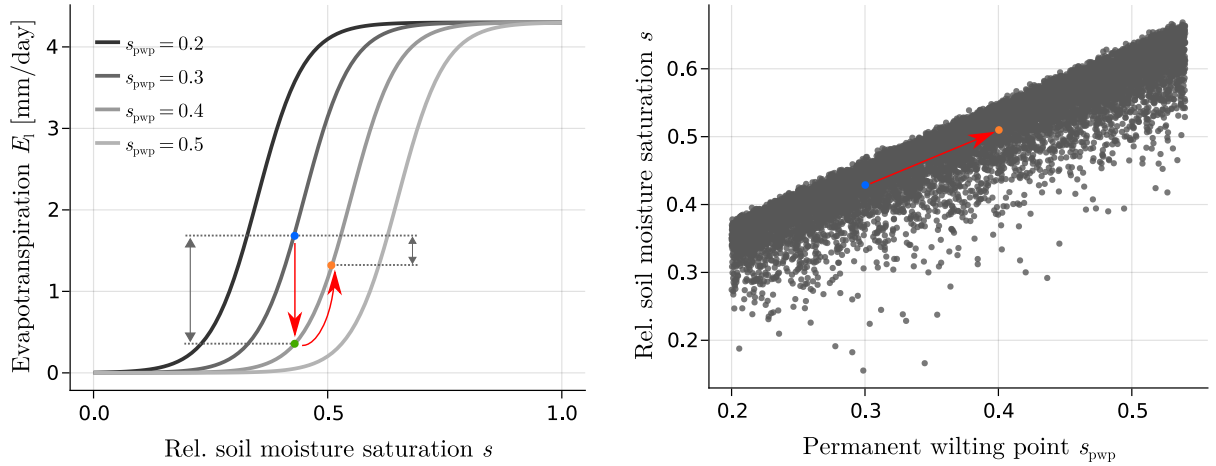


FIG. 6. Influence of an increase in s_{pwp} on the equilibrium state. Left: Higher values of s_{pwp} shift the graph of the E_l parametrization towards larger s . Right: Equilibrium values of the soil moisture saturation from CM data plotted over s_{pwp} values. In left panel, next to left black arrows will stand something like ΔE_{inst} for instantaneous ET-difference and next to the right black arrows ΔE_{eq} to denote the ET difference between old and new equilibrium state.

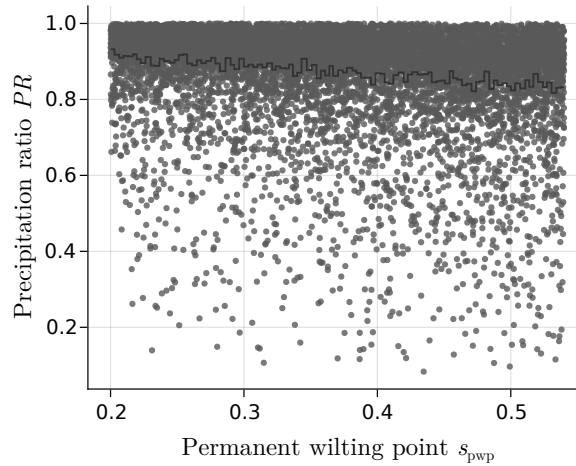


FIG. 7. s_{pwp} -dependence

The meaning of the soil moisture variable s is unchanged, while a different notation is employed for the water content of the atmospheric boxes. The index $i = 1, 2, 3$ is used to denote the mean integrated water vapour pass w_i and net advection rate A_i of the first ocean atmosphere ($i = 1$), land atmosphere ($i = 2$) and second ocean atmosphere ($i = 3$), respectively. With this, the model equations read

$$\frac{ds}{dt} = \frac{1}{nz_r} [P(w_2) - R(s, w_2) - E(s)] \quad (17)$$

$$\frac{dw_1}{dt} = e_o - P(w_1) + A_1 \quad (18)$$

$$\frac{dw_2}{dt} = E(s) - P(w_2) + A_2 \quad (19)$$

$$\frac{dw_3}{dt} = e_o - P(w_3) + A_3, \quad (20)$$

with

$$A_i = \frac{(w_{i-1} - w_i)u}{L_i}. \quad (21)$$

Note, that a new parameter w_0 was introduced which denotes the boundary condition of the water vapor pass at the windward end of the model domain. It reflects the **synoptic scale?** conditions which the model is embedded in.

b. Open model results

- How the open model relaxes the condition that $PR < 1$ ($PR > 1$ only under certain rare conditions)
- The role of synoptic moisture conditions in the atmosphere
- Open model can be transformed into the closed model

6. Discussion

- Which aspects of this study change the way we look at precipitation partitioning? (Especially, which relationships were not clear from the start?)
- Which conditions need to be met to end up with a precipitation ratio larger one, what role does a correct parametrization of precipitation play in this respect?
- What are possible use cases for the models?

- What can the model(s) tell us and what not and why? (e.g. land distribution not representative for the Tropics)
- ...

7. Conclusions

This study was motivated by our lack of theoretical understanding of how Earth's total precipitation gets partitioned between land and ocean. More precisely, we wanted to know which physical processes and quantities determine the partitioning and whether the range of plausible values for these quantities sets constraints on the ratio between spatio-temporal mean land and ocean precipitation, $PR = P_l/P_o$.

To this end, we introduce a conceptual water balance model that describes the rate of change of soil moisture and atmospheric moisture over ocean and land, respectively. Drawing inspiration from earlier works by Rodriguez-Iturbe et al. (1991) and Bretherton et al. (2004), the water balance components are expressed as functions of the mean water content of the land and atmospheric subdomains. These functions contain several environmental parameters, some of which can be assumed to stay constant on human timescales, e.g. Earth's land fraction, and others that might change in a changing climate such as mean horizontal wind speed or properties of the soil. Assuming that the Earth system's moisture state is a steady state on the timescale of a couple of years, we analyze a large number of equilibrium solutions for different combinations of model parameter values. The obtained results can be summarized as follows:

- To reach equilibrium, the fundamental property of soil to lose water through runoff demands a net atmospheric moisture transport from the ocean to the land and a runoff return flow of identical magnitude from soil to ocean. In a closed, two-domain model, the ocean atmosphere will therefore equilibrate at a moister value than the land atmosphere. If the same relationship between precipitation and atmospheric moisture holds for land and ocean regions, then the precipitation ratio is bound by an upper limit of $PR = 1$.
- The lower bound of the precipitation ratio is mostly determined by the atmospheric moisture transport parameter, $\tau = u/L$. Efficient advection (large τ) results in similar moisture conditions over land and ocean and, hence, similar precipitation rates, while inefficient advection

(low τ) leads to large moisture differences and an ocean precipitation up to ten times as strong as over land ($PR \approx 0.1$). Significant sensitivity is also found to a variation of land fraction α and to a lesser extent to the permanent wilting point and field capacity of the soil. The land fraction is most relevant near its extreme values of a large ocean and small land, $\alpha \rightarrow 0$, where the overall moisture state of the model is wet and of a small ocean and large land where the moisture state is dry. In both extreme cases, the precipitation ratio attains values close to one. In contrast, for intermediate values, the land fraction loses much of its predictive power and the influence of τ dominates.

- The conceptual water balance model has difficulties explaining observed island precipitation enhancement. Although precipitation ratios larger than one are found for an open model configuration which is more apt for simulating the spatial scales of islands, these cases of precipitation enhancement make up for only a rather small subset of the parameter space which is characterized by small land sizes, rather large water vapor pass boundary values and a tendency for small values of τ . A necessary condition for land precipitation enhancement in this model framework is a moisture cascade along the wind trajectory.

Although these findings suggest a rather strong and qualitatively robust sensitivity of precipitation partitioning to certain physical properties of the Earth system, we have to keep in mind that the employed model equations are the product of a number of strong assumptions. Foremost, we assumed the same precipitation parametrization to hold over land and ocean. It is likely that this is not justified. Knowing whether the same mean water vapour pass will result in more or less precipitation over land compared to over ocean would clarify whether the precipitation ratio can become larger than one on global scales. An appropriate observational investigation of this relationship is therefore a possible direction for future studies. Another limitation of this study that might have a qualitative influence on the inferred bounds of the precipitation ratio is the role of land distributions. Configurations with more than one land box require additional model equations and will exhibit different equilibrium states for the same choice of model parameter values compared to the two-domain model configuration.

Lastly, the pure water balance approach explored in this study is insufficient to cover the full range of physical processes that are evoked by land-ocean differences. Especially the different ways in which the two surfaces partition incoming energy into sensible and latent heat fluxes might have

543 a major indirect impacts on the partitioning of precipitation. For instance, it is plausible that sea
544 breezes could temporarily transport more moisture into the land atmosphere, causing high rain rates
545 due to the nonlinear dependence of precipitation on water vapor pass. In such a scenario, the ocean
546 atmosphere could still be moister than the land atmosphere on average but mean precipitation over
547 land might be higher even when using the same parametrization $P(w)$. Particularly in the context
548 of island precipitation enhancement, energy considerations might be indispensable. Extending
549 the model framework by energy balance equations or incorporating the effect of the diurnal cycle
550 indirectly through energy-dependent parameters promises to yield a more complete theoretical
551 understanding of precipitation partitioning.

Acknowledgments.

Data availability statement.

References

- Bretherton, C. S., M. E. Peters, and L. E. Back, 2004: Relationships between water vapor path and precipitation over the tropical oceans. *J. Climate*, **17**, 1517–1528, [https://doi.org/10.1175/1520-0442\(2004\)017<1517:RBWVPA>2.0.CO;2](https://doi.org/10.1175/1520-0442(2004)017<1517:RBWVPA>2.0.CO;2).
- Brubaker, K., D. Entekhabi, and P. Eagleson, 1991: Atmospheric water vapor transport: Estimation of continental precipitation recycling and parameterization of a simple climate model. URL <https://ntrs.nasa.gov/citations/19910018381>.
- Brubaker, K. L., D. Entekhabi, and P. S. Eagleson, 1993: Estimation of continental precipitation recycling. *Journal of Climate*, **6**, 1077–1089, [https://doi.org/10.1175/1520-0442\(1993\)006<1077:EOCPR>2.0.CO;2](https://doi.org/10.1175/1520-0442(1993)006<1077:EOCPR>2.0.CO;2), URL <https://journals.ametsoc.org/jcli/article/6/6/1077/39303/Estimation-of-Continental-Precipitation-Recycling>.
- Budyko, M. I., 1956: *Heat balance of the Earth's surface*. U.S. Dept. of Commerce, Weather Bureau.
- Budyko, M. I., and O. A. Drozdov, 1953: Characteristics of the moisture circulation in the atmosphere. **4**, 5–14.
- Burde, G. I., and A. Zangvil, 2001: The estimation of regional precipitation recycling. part i: Review of recycling models. *Journal of Climate*, **14** (12), 2497–2508, [https://doi.org/10.1175/1520-0442\(2001\)014<2497:TEORPR>2.0.CO;2](https://doi.org/10.1175/1520-0442(2001)014<2497:TEORPR>2.0.CO;2), URL <https://journals.ametsoc.org/jcli/article/14/12/2497/29526/The-Estimation-of-Regional-Precipitation-Recycling>.
- Cronin, T. W., K. A. Emanuel, and P. Molnar, 2015: Island precipitation enhancement and the diurnal cycle in radiative-convective equilibrium. **141** (689), 1017–1034, <https://doi.org/10.1002/qj.2443>, URL <https://rmets.onlinelibrary.wiley.com/doi/abs/10.1002/qj.2443>.
- Datseris, G., 2018: Dynamicalsystems.jl: A julia software library for chaos and nonlinear dynamics. *Journal of Open Source Software*, **3**, 598, <https://doi.org/10.21105/joss.00598>.

- 578 Datseris, G., and U. Parlitz, 2022: *Nonlinear Dynamics*. 2192-4791, Springer International Pub-
579 lishing, URL <https://link.springer.com/book/9783030910334>.
- 580 Eltahir, E. a. B., and R. L. Bras, 1994: Precipitation recycling in the amazon basin. *Quarterly Jour-*
581 *nal of the Royal Meteorological Society*, **120**, 861–880, <https://doi.org/10.1002/qj.49712051806>,
582 URL <https://onlinelibrary.wiley.com/doi/abs/10.1002/qj.49712051806>.
- 583 Ent, R. J. v. d., H. H. G. Savenije, B. Schaefli, and S. C. Steele-Dunne, 2010: Ori-
584 gin and fate of atmospheric moisture over continents. *Water Resources Research*, **46** (9),
585 <https://doi.org/10.1029/2010WR009127>, URL [https://agupubs.onlinelibrary.wiley.com/doi/abs/](https://agupubs.onlinelibrary.wiley.com/doi/abs/10.1029/2010WR009127)
586 [10.1029/2010WR009127](https://doi.org/10.1029/2010WR009127).
- 587 Entekhabi, D., I. Rodriguez-Iturbe, and R. L. Bras, 1992: Variability in large-scale water bal-
588 ance with land surface-atmosphere interaction. *Journal of Climate*, **5**, 798–813, [https://doi.org/](https://doi.org/10.1175/1520-0442(1992)005<0798:VILSWB>2.0.CO;2)
589 [10.1175/1520-0442\(1992\)005<0798:VILSWB>2.0.CO;2](https://doi.org/10.1175/1520-0442(1992)005<0798:VILSWB>2.0.CO;2), URL [https://journals.ametsoc.org/](https://journals.ametsoc.org/jcli/article/5/8/798/35919/Variability-in-Large-Scale-Water-Balance-with-Land)
590 [jcli/article/5/8/798/35919/Variability-in-Large-Scale-Water-Balance-with-Land](https://journals.ametsoc.org/jcli/article/5/8/798/35919/Variability-in-Large-Scale-Water-Balance-with-Land).
- 591 Fiedler, S., and Coauthors, 2020: Simulated tropical precipitation assessed across three major
592 phases of the coupled model intercomparison project (CMIP). *Monthly Weather Review*, **148** (9),
593 3653–3680, <https://doi.org/10.1175/MWR-D-19-0404.1>.
- 594 Findell, K. L., and E. A. B. Eltahir, 2003: Atmospheric controls on soil mois-
595 ture–boundary layer interactions. part i: Framework development. *Journal of Hy-*
596 *drometeorology*, **4** (3), 552–569, [https://doi.org/10.1175/1525-7541\(2003\)004<0552:](https://doi.org/10.1175/1525-7541(2003)004<0552:ACOSML>2.0.CO;2)
597 [ACOSML>2.0.CO;2](https://doi.org/10.1175/1525-7541(2003)004<0552:ACOSML>2.0.CO;2), URL [https://journals.ametsoc.org/jhm/article/4/3/552/68951/](https://journals.ametsoc.org/jhm/article/4/3/552/68951/Atmospheric-Controls-on-Soil-Moisture-Boundary)
598 [Atmospheric-Controls-on-Soil-Moisture-Boundary](https://journals.ametsoc.org/jhm/article/4/3/552/68951/Atmospheric-Controls-on-Soil-Moisture-Boundary).
- 599 Froidevaux, P., L. Schlemmer, J. Schmidli, W. Langhans, and C. Schär, 2014: Influence of
600 the background wind on the local soil moisture–precipitation feedback. *Journal of the At-*
601 *mospheric Sciences*, **71** (2), 782–799, <https://doi.org/10.1175/JAS-D-13-0180.1>, URL <https://journals.ametsoc.org/doi/10.1175/JAS-D-13-0180.1>.
602
- 603 Hagemann, S., and T. Stacke, 2015: Impact of the soil hydrology scheme on simulated soil moisture
604 memory. *Climate Dyn.*, **44**, 1731–1750, <https://doi.org/10.1007/s00382-014-2221-6>.

605 Hohenegger, C., P. Brockhaus, C. S. Bretherton, and C. Schär, 2009: The soil mois-
 606 ture–precipitation feedback in simulations with explicit and parameterized convection. *Journal*
 607 *of Climate*, **22** (19), 5003–5020, <https://doi.org/10.1175/2009JCLI2604.1>, URL [https://journals.](https://journals.ametsoc.org/jcli/article/22/19/5003/32298/The-Soil-Moisture-Precipitation-Feedback-in)
 608 [ametsoc.org/jcli/article/22/19/5003/32298/The-Soil-Moisture-Precipitation-Feedback-in](https://journals.ametsoc.org/jcli/article/22/19/5003/32298/The-Soil-Moisture-Precipitation-Feedback-in).

609 Hohenegger, C., and B. Stevens, 2018: The role of the permanent wilting point in controlling the
 610 spatial distribution of precipitation. *Proceedings of the National Academy of Sciences*, **115** (22),
 611 5692–5697, <https://doi.org/10.1073/pnas.1718842115>, URL [https://www.pnas.org/content/115/](https://www.pnas.org/content/115/22/5692)
 612 [22/5692](https://www.pnas.org/content/115/22/5692).

613 Lynn, B. H., W.-K. Tao, and P. J. Wetzel, 1998: A study of landscape-generated
 614 deep moist convection. *Monthly Weather Review*, **126** (4), 928–942, [https://doi.org/](https://doi.org/10.1175/1520-0493(1998)126<0928:ASOLGD>2.0.CO;2)
 615 [10.1175/1520-0493\(1998\)126<0928:ASOLGD>2.0.CO;2](https://doi.org/10.1175/1520-0493(1998)126<0928:ASOLGD>2.0.CO;2), URL [https://journals.ametsoc.org/](https://journals.ametsoc.org/mwr/article/126/4/928/66256/A-Study-of-Landscape-Generated-Deep-Moist)
 616 [mwr/article/126/4/928/66256/A-Study-of-Landscape-Generated-Deep-Moist](https://journals.ametsoc.org/mwr/article/126/4/928/66256/A-Study-of-Landscape-Generated-Deep-Moist).

617 Manabe, S., 1969: CLIMATE AND THE OCEAN CIRCULATION: I. THE ATMOSPHERIC
 618 CIRCULATION AND THE HYDROLOGY OF THE EARTH’S SURFACE. *Monthly Weather*
 619 *Review*, **97** (11), 739–774, [https://doi.org/10.1175/1520-0493\(1969\)097<0739:CATOC>2.](https://doi.org/10.1175/1520-0493(1969)097<0739:CATOC>2.3.CO;2)
 620 [3.CO;2](https://doi.org/10.1175/1520-0493(1969)097<0739:CATOC>2.3.CO;2), URL [https://journals.ametsoc.org/view/journals/mwre/97/11/1520-0493_1969_097_](https://journals.ametsoc.org/view/journals/mwre/97/11/1520-0493_1969_097_0739_catoc_2_3_co_2.xml)
 621 [0739_catoc_2_3_co_2.xml](https://journals.ametsoc.org/view/journals/mwre/97/11/1520-0493_1969_097_0739_catoc_2_3_co_2.xml).

622 Peixóto, J. P., and A. H. Oort, 1983: The atmospheric branch of the hydrological cycle and
 623 climate. *Variations in the Global Water Budget*, Springer Netherlands, 5–65, [https://doi.org/](https://doi.org/10.1007/978-94-009-6954-4_2)
 624 [10.1007/978-94-009-6954-4_2](https://doi.org/10.1007/978-94-009-6954-4_2), URL https://doi.org/10.1007/978-94-009-6954-4_2.

625 Qian, J.-H., 2008: Why precipitation is mostly concentrated over islands in
 626 the maritime continent. *Journal of the Atmospheric Sciences*, **65** (4), 1428–
 627 1441, <https://doi.org/10.1175/2007JAS2422.1>, URL [https://journals.ametsoc.org/jas/article/65/](https://journals.ametsoc.org/jas/article/65/4/1428/26793/Why-Precipitation-Is-Mostly-Concentrated-over)
 628 [4/1428/26793/Why-Precipitation-Is-Mostly-Concentrated-over](https://journals.ametsoc.org/jas/article/65/4/1428/26793/Why-Precipitation-Is-Mostly-Concentrated-over).

629 Rodriguez-Iturbe, I., D. Entekhabi, and R. L. Bras, 1991: Nonlinear dynamics of soil moisture at
 630 climate scales: 1. stochastic analysis. *Water Resources Research*, **27**, 1899–1906, [https://doi.org/](https://doi.org/10.1029/91WR01035)
 631 [10.1029/91WR01035](https://doi.org/10.1029/91WR01035).

632 Schär, C., D. Lüthi, U. Beyerle, and E. Heise, 1999: The soil–precipitation feedback:
 633 A process study with a regional climate model. *Journal of Climate*, **12** (3), 722–741,
 634 [https://doi.org/10.1175/1520-0442\(1999\)012<0722:TSPFAP>2.0.CO;2](https://doi.org/10.1175/1520-0442(1999)012<0722:TSPFAP>2.0.CO;2), URL [https://journals.](https://journals.ametsoc.org/jcli/article/12/3/722/28833/The-Soil-Precipitation-Feedback-A-Process-Study)
 635 [ametsoc.org/jcli/article/12/3/722/28833/The-Soil-Precipitation-Feedback-A-Process-Study](https://journals.ametsoc.org/jcli/article/12/3/722/28833/The-Soil-Precipitation-Feedback-A-Process-Study).

636 Segal, M., and R. W. Arritt, 1992: Nonclassical mesoscale circulations caused by
 637 surface sensible heat-flux gradients. *Bulletin of the American Meteorological Society*,
 638 **73** (10), 1593–1604, [https://doi.org/10.1175/1520-0477\(1992\)073<1593:NMCCBS>2.0.CO;](https://doi.org/10.1175/1520-0477(1992)073<1593:NMCCBS>2.0.CO;2)
 639 2, URL [https://journals.ametsoc.org/view/journals/bams/73/10/1520-0477_1992_073_1593_](https://journals.ametsoc.org/view/journals/bams/73/10/1520-0477_1992_073_1593_nmccbs_2_0_co_2.xml)
 640 [nmccbs_2_0_co_2.xml](https://journals.ametsoc.org/view/journals/bams/73/10/1520-0477_1992_073_1593_nmccbs_2_0_co_2.xml).

641 Seneviratne, S. I., T. Corti, E. L. Davin, M. Hirschi, E. B. Jaeger, I. Lehner, B. Orlowsky, and
 642 A. J. Teuling, 2010: Investigating soil moisture–climate interactions in a changing climate:
 643 A review. **99** (3), 125–161, <https://doi.org/10.1016/j.earscirev.2010.02.004>, URL [https://www.](https://www.sciencedirect.com/science/article/pii/S0012825210000139)
 644 [sciencedirect.com/science/article/pii/S0012825210000139](https://www.sciencedirect.com/science/article/pii/S0012825210000139).

645 Shannon, C. E., 1948: A mathematical theory of communication. *The Bell System Technical*
 646 *Journal*, **27** (3), 379–423, <https://doi.org/10.1002/j.1538-7305.1948.tb01338.x>.

647 Sobel, A. H., C. D. Burleyson, and S. E. Yuter, 2011: Rain on small tropical islands. *Journal of*
 648 *Geophysical Research: Atmospheres*, **116**, <https://doi.org/10.1029/2010JD014695>, URL [https:](https://agupubs.onlinelibrary.wiley.com/doi/abs/10.1029/2010JD014695)
 649 [//agupubs.onlinelibrary.wiley.com/doi/abs/10.1029/2010JD014695](https://agupubs.onlinelibrary.wiley.com/doi/abs/10.1029/2010JD014695).

650 Ulrich, M., and G. Bellon, 2019: Superenhancement of precipitation at the center of tropical islands.
 651 *Geophysical Research Letters*, **46** (24), 14 872–14 880, <https://doi.org/10.1029/2019GL084947>,
 652 URL <https://agupubs.onlinelibrary.wiley.com/doi/abs/10.1029/2019GL084947>.

653 Wang, S., and A. H. Sobel, 2017: Factors controlling rain on small tropical islands: Diurnal cycle,
 654 large-scale wind speed, and topography. *Journal of the Atmospheric Sciences*, **74** (11), 3515–
 655 3532, <https://doi.org/10.1175/JAS-D-16-0344.1>, URL [https://journals.ametsoc.org/jas/article/](https://journals.ametsoc.org/jas/article/74/11/3515/42168/Factors-Controlling-Rain-on-Small-Tropical-Islands)
 656 [74/11/3515/42168/Factors-Controlling-Rain-on-Small-Tropical-Islands](https://journals.ametsoc.org/jas/article/74/11/3515/42168/Factors-Controlling-Rain-on-Small-Tropical-Islands).

657 Zangvil, A., D. H. Portis, and P. J. Lamb, 1993: Diurnal variations in the water vapor bud-
 658 get components over the midwestern united states in summer 1979. *Interactions Between*

659 *Global Climate Subsystems*, American Geophysical Union (AGU), 53–63, [https://doi.org/](https://doi.org/10.1029/GM075p0053)
660 10.1029/GM075p0053, URL <https://onlinelibrary.wiley.com/doi/abs/10.1029/GM075p0053>.